Axonal netrin-Gs transneuronally determine lamina-specific subdendritic segments

Sachiko Nishimura-Akiyoshi*, Kimie Niimi[†‡], Toshiaki Nakashiba*[§], and Shigeyoshi Itohara*[¶]

*Laboratory for Behavioral Genetics and [†]Research Resources Center, RIKEN Brain Science Institute, 2-1 Hirosawa, Wako, Saitama 351-0198, Japan; [‡]Brain Science and Life Technology Research Foundation, 1-28-12 Narimasu, Itabashi, Tokyo 175-0094, Japan; and [§]The Picower Institute for Learning and Memory, RIKEN-MIT Neuroscience Research Center, Massachusetts Institute of Technology, Cambridge, MA 02139

Communicated by Susumu Tonegawa, Massachusetts Institute of Technology, Cambridge, MA, July 24, 2007 (received for review December 27, 2006)

Axons from a distinct group of neurons make contact with dendritic trees of target neurons in clearly segregated and laminated patterns, thereby forming functional units for processing multiple inputs of information in the vertebrate central nervous system. Whether and how dendrites acquire lamina-specific properties corresponding to each pathway is not known. We show here that vertebrate-specific membrane-anchored members of the UNC-6/netrin family, netrin-G1 and -G2, organize the lamina/pathway-specific differentiation of dendrites. Netrin-G1 and -G2 distribute on axons of different pathways and specifically interact with receptors NGL-1 and -2, respectively. In the hippocampus, parietal cortex, and piriform cortex, NGL-1 is concentrated in the dendritic segments corresponding to the lamina-specific termination of netrin-G1-positive axons, and NGL-2 is concentrated in distinct dendritic segments corresponding to the termination of netrin-G2-positive axons. In netrin-G1- and -G2-deficient mice, in which axonal path-finding is normal, the segmental distribution of NGL-1 and -2 is selectively disrupted, and the individual receptors are diffused along the dendrites. These findings indicate that transneuronal interactions of netrin-Gs and their specific receptors provide a molecular basis for the axonal innervation-dependent mechanism of postsynaptic membrane organization, and provide insight into the formation of the laminar structure within the dendrites.

cortical layer | neuronal circuit | protein–protein interaction

One remarkable feature of the vertebrate central nervous system is its cortical laminar structure. In addition to the layered distribution of different types of neurons, distinct populations of axons originating from multiple brain areas innervate distinct laminae. In cases where distinct axons project to a single neuron, they synapse onto distinct subcellular compartments (dendrite, soma, and axon initial segment), and in many cases, restricted segments within target dendrites (1). In mammalian hippocampus, for example, extrinsic inputs from the entorhinal cortex (EC) terminate on distal parts of the hippocampal neuronal dendrites, whereas fibers of inter- or intrahippocampal projections terminate on the proximal parts of dendrites in a laminated manner with sharp boundaries (2). Such lamina-specific connectivity along a dendrite might be the structural basis for organized processing and integration of multiple inputs. Various axon guidance molecules are implicated in the lamina-specific targeting of axons (3).

Despite the well characterized laminar organization of presynaptic fibers, little is known about the lamina-specific properties of dendrites. Some electrophysiologic and immunolocalization studies demonstrated that dendrites originating from the same neuron possess distinct properties depending on the site, such as different neurotransmitter receptor compositions (4, 5), voltage-gated channel densities (6), and synapse morphology (7). However, these experiments were performed with very limited cell types, such as the CA1 pyramidal neuron, and thus it is unclear whether the uneven distribution of postsynaptic machinery within the dendritic trees is a general feature of neurons. The mechanisms that might underlie the spatial organization of these dendritic properties are also unknown.

Netrin-G1 and -G2 (also called laminet-1 and -2) comprise a subfamily within the UNC-6/netrin family (8–10). Classic netrins are phylogenetically conserved, diffusible chemoattractants of axon guidance molecules (11–13). Unlike classic netrins, netrin-Gs are linked to the plasma membrane surface by a glycosylphosphatidylinositol linkage, have no orthologues in invertebrates and lack affinity to the known netrin receptor families, DCC and Unc5h (8, 9). Instead, netrin-G1 binds to a cell adhesion molecule NGL-1 (14), and netrin-G2 binds to another NGL family protein, NAG14[‖]. NGL-2 (also known as NAG14 and referred to here as NGL-2) is preferentially localized to the postsynaptic side in association with PSD-95, and has bidirectional synaptogenic activity in cell culture systems (15). Both netrin-G1 and -G2 are predominantly expressed in the brain, and each is expressed in distinct subsets of neurons in a complementary manner (9, 10). These findings suggest that the roles of the netrin-G subfamily members are different from those of classic netrins, and that they contribute to the elaboration of the complex and highly organized nervous systems unique to vertebrates.

The findings of the present study indicated that netrin-G1 and -G2 proteins are selectively distributed on axons of distinct pathways and transneuronally interact with the receptor proteins NGL-1 and -2, respectively, on target dendrites. The distribution of netrin-G1/NGL-1 and netrin-G2/NGL-2 adhesion couples was closely associated with the lamina-specific connectivity of several neural pathways. Loss-of-function studies in mice revealed that netrin-G1 and -G2 confine the localization of their specific receptors to discrete subdendritic segments in a pathway-specific manner. These findings suggest an instructive role for axon-derived factors in the segmental differentiation of target dendrites.

Results

Pathway-Specific Distribution of Netrin-G1 and -G2 Proteins in the Mouse Brain. The netrin-G1 (*Ntng1*) and netrin-G2 (*Ntng2*) genes are expressed in the mouse brain in a complementary manner; e.g., *Ntng1* in the dorsal thalamus and olfactory bulb, and *Ntng2* in the cerebral cortex (9, 10). In the present study, immunohis-

Author contributions: S.N.-A., T.N., and S.I. designed research; S.N.-A. and K.N. performed research; S.N.-A., K.N., and S.I. contributed new reagents/analytic tools; S.N.-A. and S.I. analyzed data; and S.N.-A., T.N., and S.I. wrote the paper.

The authors declare no conflict of interest.

Freely available online through the PNAS open access option.

Abbreviations: DG, dentate gyrus; EC, entorhinal cortex; LPP, lateral perforant path; MPP, medial perforant path; TA, temporoammonic pathway; KO, knockout.

[¶]To whom correspondence should be addressed. E-mail: sitohara@brain.riken.jp.

[‖]Nishimura, S., Niimi, K., Hashikawa, T., Nakashiba, T., Itohara, S. (2005) *Soc Neurosci Abstr*, Program no. 601.4 (abstr.).

This article contains supporting information online at www.pnas.org/cgi/content/full/0706919104/DC1.

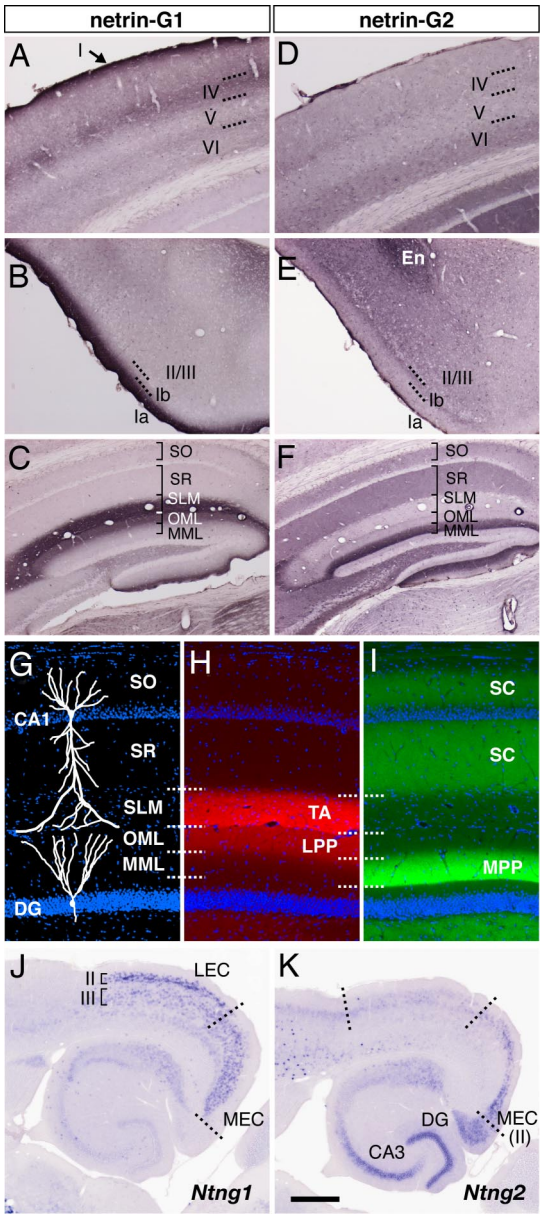

Fig. 1. Selective distribution of netrin-G1 and -G2 proteins in distinct pathways. Coronal sections of adult mouse brain were stained with anti-netrin-G1 (*A–C*) and anti-netrin-G2 antibodies (*D–F*). Netrin-G1 and -G2 had a nonoverlapping and layer-specific distribution in the neocortex, piriform cortex, and hippocampus. Laminar organization (*G*), and distribution of netrin-G1 (*H*) and netrin-G2 (*I*) in the hippocampus. Netrin-G1 immunoreactivity was restricted to the terminal layers of the lateral perforant paths (LPP) in the DG and TA in CA1, whereas netrin-G2 was restricted to the terminal layers of the medial perforant paths (MPP) and SC. En, endopiriform nucleus; MML, middle molecular layer; OML, outer molecular layer; SLM, stratum lacunosum moleculare; SO, stratum oriens; SR, stratum radiatum. (*J* and *K*) Serial horizontal sections were hybridized with digoxigenin-labeled RNA probes. Note the complementary expression of *Ntng1* and *Ntng2* mRNAs in the LEC and MEC. [Scale bar: 200 μm (*A* and *D*); 250 μm (*B*, *C*, *E*, and *F*); 140 μm (*G–I*); 500 μm (*J* and *K*).]

tochemistry of netrin-G1 and -G2 revealed that these two proteins were differentially distributed in a laminated manner in several regions of the adult mouse brain.

In the parietal region of the neocortex, netrin-G1 was detected in layers I and IV with intense staining, and at the border of layer V/VI with faint staining (Fig. 1*A*). These patterns correspond to the terminal arborization of thalamocortical axons (16). In the piriform cortex, netrin-G1 was strongly detected in layer Ia (Fig. 1*B*), which is the terminal layer of mitral cell axons from the olfactory bulb (17). These data are consistent with previous reports of axonal localization of netrin-G1 in the developing brain [see supporting information (SI) Fig. 6] (9, 18). Netrin-G2 was detected in layers VI and IV of the parietal cortex (Fig. 1*D*), in layer Ib and deeper layers of the piriform cortex, and in the endopiriform nucleus (Fig. 1*E*). As *Ntng2* transcripts are abundant in the cerebral cortex and primary olfactory cortex (9, 10), netrin-G2 proteins are most likely distributed on intracortical projections.

In the hippocampus, there was a mutually exclusive distribution of netrin-Gs. Netrin-G1 immunoreactivity was clearly detected in the outer-third of the molecular layer of the dentate gyrus (DG) and in the stratum lacunosum moleculare of CA1 (Fig. 1*C*). In contrast, there was strong staining of netrin-G2 in the middle-third of the molecular layer of the DG and in the stratum radiatum and stratum oriens of CA1 (Fig. 1*F*). These patterns correspond well to the lamina-specific termination of hippocampal circuits. In the DG, the LPP and MPP arising from layer II neurons of the lateral and medial entorhinal cortex (LEC and MEC) terminate on the outer and middle molecular layer, respectively. In the CA1, the temporoammonic (TA) pathway originating from layer III neurons of the EC terminates on the stratum lacunosum-moleculare, whereas the Schaffer collaterals (SC) from CA3 neurons terminate on the stratum radiatum and stratum oriens (Fig. 1 *G–I*) (19). Indeed, *Ntng1* mRNA levels were high in layer II of the LEC (origin of the LPPs) and layer III throughout the EC (origin of the TA), but very low in the dentate granule cells and pyramidal neurons of the hippocampus (target cells of the LPPs and TA, respectively, Fig. 1*J*). In marked contrast, *Ntng2* mRNA was selectively detected in layer II of the MEC (origin of the MPPs), consistent with the netrin-G2 distribution in the middle molecular layer of the DG (Fig. 1*K*). *Ntng2* mRNA was also detected in the DG (target of the MPPs). Netrin-G2 antibody labeled the areas representing mossy fiber tracts from the DG to CA3, but not the outer or innermost part of the DG molecular layer (SI Fig. 7), and therefore netrin-G2 protein seems to be preferentially distributed on axons rather than on the DG dendrites. With respect to the CA3-CA1 pathway (SC), *Ntng2* mRNA was abundant in CA3, but very low in the target CA1 pyramidal neurons (Fig. 1*K*). These selective expression patterns in presynaptic neurons indicate that netrin-G1 and -G2 proteins are distributed on different populations of axons in a pathway-specific manner.

Specific Binding of Netrin-G1 and -G2 with NGL-1 and -2. Netrin-G1 interacts with a cell adhesion molecule, NGL-1 (14). In the mouse databases, there are two additional related molecules: NGL-2 and -3 (also called HSM), and we preliminarily reported that netrin-G2 selectively binds to NGL-2[‖]. Here, we evaluated their binding specificities. Netrin-G1 bound to NGL-1 (Fig. 2*A*), but not to NGL-2 or -3-expressing cells (Fig. 2*B* and data not shown). In contrast, netrin-G2 bound to NGL-2 (Fig. 2*D*), but not to NGL-1 or -3 (Fig. 2*C* and data not shown). Additionally, classic netrin-1 did not bind to any NGL family member (ref. 14 and data not shown). These specific interactions were further confirmed by binding affinity measurements using the BIAcore system. The K_d values of netrin-G1/NGL-1 and netrin-G2/NGL-2 interactions were 1.55×10^{-7} M and 3.27×10^{-7} M, respectively (Fig. 2 *E* and *F*). The cross-reactivity of other ligand–receptor combinations was below the detection limits of the system. These results suggest that netrin-G1 and -G2 interact with distinct members of the receptor protein family NGLs, and therefore have nonredundant functions. Kim *et al.* (15) independently obtained similar but qualitative data.

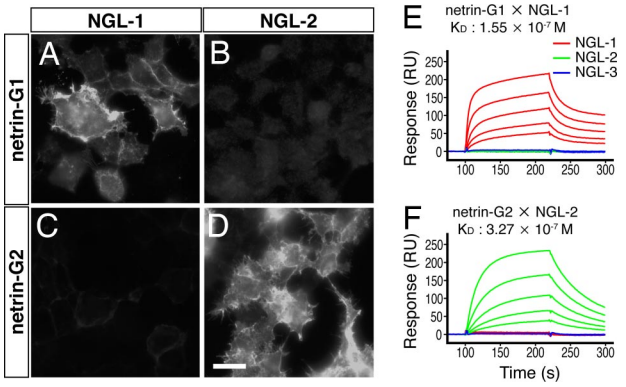

Fig. 2. Differential binding of netrin-G1 and -G2 to the NGL family proteins. Recombinant myc-tagged proteins of mouse netrin-G1 and -G2 were added to the HEK293T cells expressing NGLs. Surface binding of ligands was immunocytochemically detected with anti-myc antibody. Netrin-G1 specifically bound to NGL-1 (*A*), but not NGL-2-expressing cells (*B*). In contrast, netrin-G2 bound to NGL-2-expressing cells (*D*) without affinity to NGL-1 (*C*) (Scale bar: 20 μm). Binding of serially diluted netrin-G1 (*E*) and netrin-G2 (*F*) proteins to the sensorchip derivatized with NGL proteins was monitored by BIAcore biosensor, and affinities (K_d) of the interaction were determined.

Selective Localization of NGL-1 and -2 in Distinct Dendritic Segments. We next examined the *in vivo* localization of NGL proteins using specific antibodies against NGL-1 and -2. Immunohistochemistry of adult mouse brain revealed distribution patterns of NGL-1 almost identical to those of netrin-G1. In the hippocampus, NGL-1 immunostaining was detected predominantly in the stratum lacunosum moleculare of CA1 (Fig. 3*A*) and faintly but significantly in the outer molecular layer of the DG (Fig. 3 *A* and *B*). In other regions, NGL-1 was restricted to specific laminae, such as layers I and IV and the boundary of layer V/VI in the parietal cortex (Fig. 3*E*) and layer Ia in the piriform cortex (Fig. 3*F*), similar to the netrin-G1 distribution shown in Fig. 1. Furthermore, the anti-NGL-2 antibody had exactly the same staining pattern as netrin-G2 in the hippocampus: the stratum radiatum and stratum oriens in the CA1 and the middle molecular layer in the DG (Fig. 3*C*). At a higher magnification, NGL-2 was identified on transversely oriented fibers in these laminae, representing the dendritic branches of the hippocampal neurons (Fig. 3*D*).

Consistent with the postsynaptic localization of NGL proteins (15), *Ngl1* and *Ngl2* mRNAs were abundant in hippocampal pyramidal neurons and dentate granule cells (the receptive neurons of the TA, SC, LPP, and MPP; Fig. 3 *G* and *H*). *Ngl1* mRNA was also highly expressed in the neocortex (the target of thalamic axons, Fig. 3*I*) and piriform cortex (the target of olfactory mitral cell axons; Fig. 3*K*), but scarcely in the dorsal thalamus (Fig. 3*J*) or olfactory bulb (Fig. 3*L*). *Ngl1* and *Ngl2* were therefore expressed in the postsynaptic neurons to which netrin-G-expressing axons project, and the immunohistochemical colocalization suggests a transneuronal interaction of axonal netrin-Gs and their specific partner NGLs on the corresponding part of the dendrites.

Generation of Netrin-G Deficient Mice. To analyze *in vivo* functions of netrin-Gs, we generated two lines of mutant mice devoid of netrin-G1 or -G2 (Fig. 4 *A* and *B*). Homozygous mutants of each line (*Ntng1* KO and *Ntng2* KO) completely lacked the gene products (Fig. 4 *D* and *H* and SI Fig. 8), and the loss of one of the netrin-G genes did not change the expression pattern of the other (Fig. 4 *E* and *G* and SI Fig. 8). Thus, netrin-G1 and -G2 appear to have independent roles in distinct groups of neurons and do not compensate for each other. Both *Ntng1* knockout (KO) and *Ntng2* KO mice developed to adults.

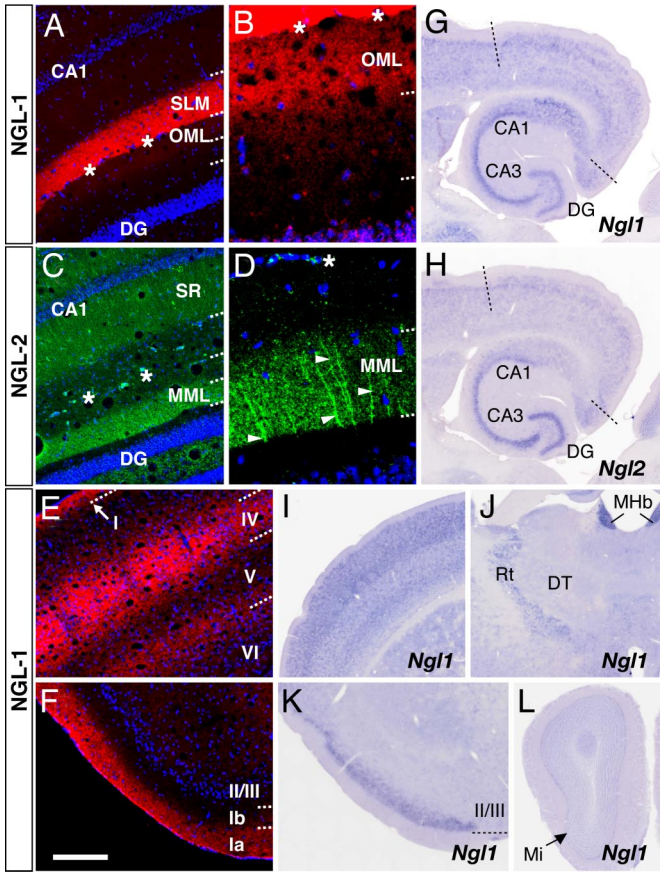

Fig. 3. Selective distribution of NGL-1 and -2 to distinct dendritic segments. Coronal sections of adult mouse brain were stained with anti-NGL-1 (*A*, *B*, *E*, and *F*) and anti-NGL-2 antibodies (*C* and *D*). NGL-1 proteins were detected in specific layers of the hippocampus [*A* and *B* (magnified image of the DG)], neocortex (*E*), and piriform cortex (*F*) with patterns similar to those of netrin-G1. (*C*) The lamina-selective distribution of NGL-2 proteins in hippocampus matches that of netrin-G2. (*D*) Dendritic staining of NGL-2 (arrowheads) at high magnification. Asterisks indicate the hippocampal fissure. (*G* and *H*) *In situ* hybridization analysis of horizontal brain sections revealed high expression levels of *Ngl1* and *Ngl2* mRNAs in pyramidal neurons of CA1-CA3 and granule cells of the DG. (*I–L*) Expression sites of *Ngl1* in other regions. *Ngl1* transcripts were abundant in the neocortex (*I*) and piriform cortex (*K*), but very low in the dorsal thalamus (DT; *J*) and olfactory bulb (*L*). MHb, medial habenular nucleus; Mi, mitral cell layer; Rt, reticular thalamic nucleus. [Scale bar: 200 μm (*A*, *C*, *E*, and *F*); 50 μm (*B* and *D*); 690 μm (*G* and *H*); 750 μm (*I* and *J*); 605 μm (*K*); 820 μm (*L*).]

Because netrin-G1 distributed on developing axons (9, 18), we tested the cell-autonomous functions of netrin-Gs for axonal development, with a focus on the thalamocortical, entorhinohippocampal, and olfactory projections (SI Fig. 9 and data not shown). There were no notable differences in the outgrowth, trajectory, area- and layer-specific terminations, and whisker lesion-induced rearrangement of the thalamocortical axons between wild-type and *Ntng1* KO mice during the first two postnatal weeks. Anterograde labeling of the perforant paths and olfactory mitral cell axons revealed lamina-specific and clearly demarcated terminations of axons in the netrin-G mutants as in wild-type mice. These histologic analyses suggest that netrin-Gs have no major roles in the gross cytoarchitecture of the brain or axonal projection.

Diffusion of Receptors Within Dendrites in Netrin-G Mutant Mice. In *Ntng1* KO and *Ntng2* KO mice, we examined whether the lack of netrin-Gs influenced the segmental dendritic distribution of

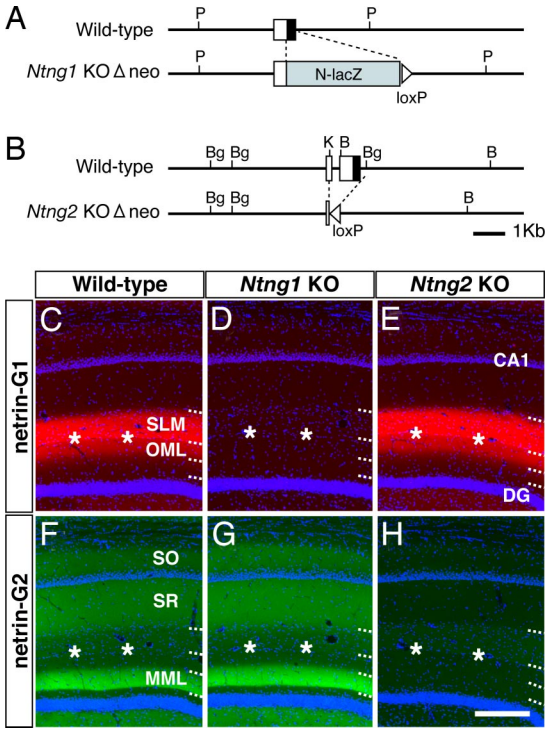

Fig. 4. Targeted disruption of netrin-G1 and -G2 genes. Schematic representation of the wild-type and mutated locus of the *Ntng1* (*A*) and *Ntng2* genes (*B*). Open boxes denote the 5′ UTR and filled boxes indicate the coding region. The *pgk-neo* cassette flanked by *loxP* sequences was excised by crossing with transgenic mice expressing Cre recombinase (Δneo). B, BamHI; Bg, BglII; K, KpnI; P, PstI. Immunohistochemistry of netrin-G1 (*C–E*) and netrin-G2 (*F–H*) in the hippocampus revealed null mutation of the targeted netrin-G and no compensatory expression of the other in each mutant line. (Scale bar: 200 μm.)

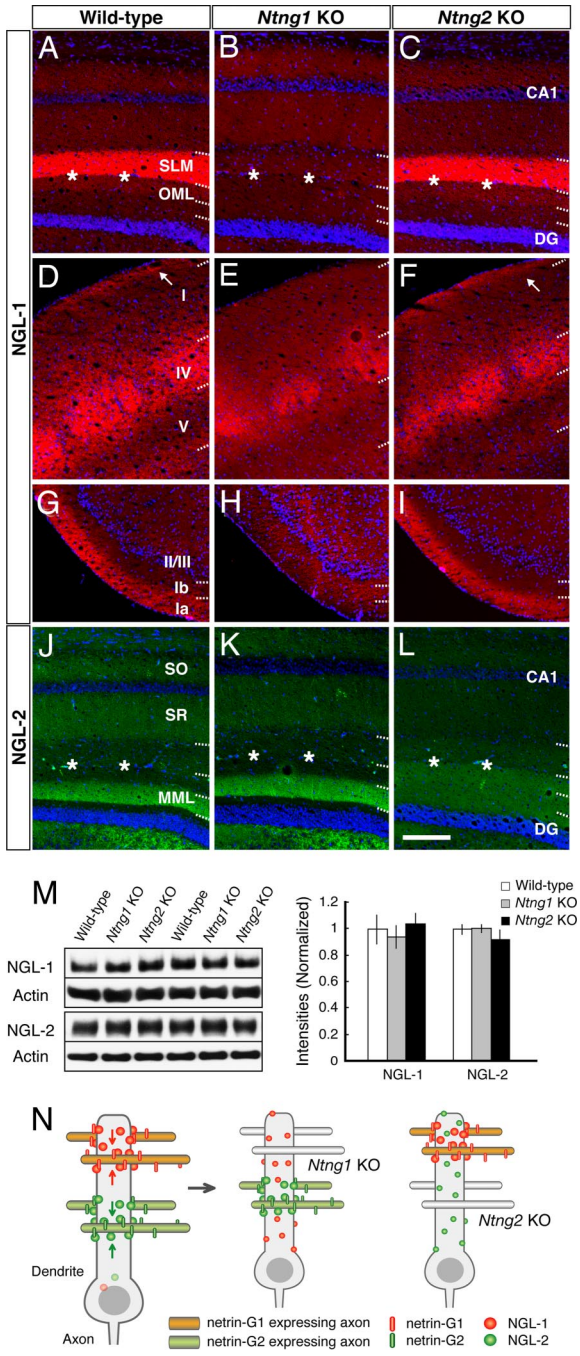

Fig. 5. Loss of lamina-restricted distribution of NGLs in netrin-G-deficient mice. Distribution patterns of NGL-1 (*A–I*) and NGL-2 (*J–L*) in wild-type and netrin-G mutant mice are shown by immunohistochemistry. Lamina-specific staining of NGL-1 was absent in *Ntng1* KO hippocampus (*B*), neocortex layer I (*E*), and piriform cortex (*H*). Similarly, there was no laminar distribution of NGL-2 in *Ntng2* KO hippocampus. Note the molecular layer of the DG, which is evenly stained with NGL-2 (*L*). Asterisks indicate the hippocampal fissure. [Scale bar: 200 μm (*A–F* and *J–L*); 250 μm (*G–I*).] (*M*) Western blot analysis of NGLs in hippocampus of wild-type, *Ntng1* KO, and *Ntng2* KO mice ($n = 4$ for each genotype) did not reveal any significant differences in the receptor protein levels, indicating a mislocation of, but not a decrease in, receptors in the mutant hippocampus. Data are presented as mean ± SEM. (*N*) Model for transneuronal regulation of receptor localization by axonal netrin-G proteins. Distinct axon populations, each expressing netrin-G1 or -G2, make contact with distinct segments of dendrites of target neurons. NGL-1 and -2, which are expressed in the target neurons, are anchored by axon-derived netrin-G1 and -G2, and are thereby precisely arranged onto the selected subdendritic segments. Without netrin-Gs as extrinsic cues, NGLs would be dispersed across multiple segments of dendrites.

their receptors. NGL-1 immunoreactivity was concentrated in specific layers in wild-type (Fig. 5 *A*, *D*, and *G*) and *Ntng2* KO brain (Fig. 5 *C*, *F*, and *I*). These patterns were absent in *Ntng1* KO hippocampus (Fig. 5*B*), layer I of the parietal cortex (Fig. 5*E*), and layer Ia of the piriform cortex (Fig. 5*H*). Similarly, lamina-selective distribution of NGL-2 was observed in wild-type and *Ntng1* KO hippocampus (Fig. 5 *J* and *K*), but lost in *Ntng2* KO mice (Fig. 5*L*). It should be noted that NGL-2 immunoreactivity in *Ntng2* KO mice was uniform across layers and was also detected in the outer and innermost part of the DG molecular layer (Fig. 5*L*). These observations suggest that the altered laminar staining patterns of NGLs are due to diffuse localization. Western blot analysis of hippocampal membrane fractions revealed no quantitative differences in receptor protein levels among the three genotypes (each genotype, $n = 4$; Fig. 5*M*). Thus, netrin-G1 and -G2 determine the proper positioning of the cognate receptor, and loss of netrin-Gs resulted in diffusion of the receptors along the dendrites of hippocampal neurons. Staining of NGL-1 in *Ntng1* KO hippocampus was very weak. This might be because of differences in the dendritic shaft size (i.e., surface area) between layers in CA1. Dendritic shafts in the stratum radiatum are quite large compared with those in the stratum lacunosum moleculare. Thus, diffusion of NGL-1 to the entire CA1 dendritic area would dilute the signal. Diffusion of NGL-1 was observed in layer I, but not layer IV of the *Ntng1* KO neocortex (Fig. 5*E*). Cortical pyramidal neurons extend their dendrites across multiple layers, whereas granule cells in layer IV confine their dendrites within layer IV. This anatomic property of layer IV cells might explain why the NGL-1 distribution in layer IV was retained in the *Ntng1* KO neocortex.

Discussion

The laminar organization observed in various regions of the vertebrate nervous system serves as a fundamental structure for processing and integrating neural information. In the present study, we first demonstrated that cell surface proteins of the UNC-6/netrin family, netrin-G1 and -G2, are localized on axons of distinct pathways, which show laminated termination in several brain regions. The distribution patterns correlate closely with the known circuitry of the cerebral cortex, olfactory cortex, and hippocampus. Second, netrin-G1 and -G2 selectively interact with distinct receptors, NGL-1 and -2, respectively. NGL-1 and -2 in the mouse brain are concentrated in distinct segments within dendrites, corresponding to the termination of axons expressing netrin-G1 and -G2, respectively. These findings reveal that the molecular composition is heterogeneous, even within the same dendrite, and that dendrites are divided into multiple compartments: ''subdendritic segments'' in a pathway-specific manner. Finally, netrin-G1 and -G2 deficient mice have selective mislocation of the individual receptors without axonal mistargeting. On the basis of these findings, we propose a model that axonal netrin-Gs ''lock in'' their specific receptors at the site of contact to localize them in the appropriate subdendritic segments (Fig. 5*N*). In the absence of netrin-G1 or -G2, NGL-1 or NGL-2 localization is ''unlocked'' and therefore the receptor diffuses along the entire dendrite. This model suggests that axonal innervation has an instructive role in dendritic segmentation. The specific netrin-G/NGL interactions are observed in various cortical regions, suggesting that our model might apply to a variety of cell types as a fundamental mechanism for forming the laminar organization of dendrites.

Because netrin-Gs are distributed on developing axons and are structurally similar to classic netrins, it is plausible that netrin-Gs also have a role in axon guidance through interaction with NGLs. Consistent with this notion, Lin *et al.* reported that immobilized NGL-1 protein promotes neurite extension in cultured neurons and that soluble NGL-1 disrupts the growth of thalamic axons in chick embryos (14). In our loss-of-function analysis of netrin-G1 and -G2, however, there were no remarkable developmental abnormalities detected in thalamocortical, entorhino-hippocampal, or olfactory projections. The discrepancy in these results might reflect species-specific differences, compensatory mechanisms, or subtle deficits in KO animals, or alternatively imply that an unidentified cofactor of netrin-G1 mediates the axon growth-promoting activity of NGL-1.

Our data indicate that netrin-G proteins transneuronally determine local dendritic properties through their receptors on dendrites after completion of axonal projection. An ankyrin-based membrane skeleton determines the localization of cell adhesion molecules in the axon initial segment of postsynaptic neurons, and thereby directs presynaptic innervation by inhibitory neurons (20). It is conceivable that such a cell-autonomous mechanism defining subcellular compartments is also used in each dendritic subregion. However, our data from netrin-G-deficient mice indicate that the segmental layout of receptors within dendrites is controlled by axonal proteins (extrinsic factors). This finding is reminiscent of the modulatory effects of nerve-derived factors on postsynaptic differentiation in the neuromuscular junction (21, 22). In the central nervous system, there are some transsynaptic adhesion molecules that induce postsynaptic differentiation. The ephrin-B/EphB interaction promotes clustering of the NMDA-type glutamate receptors to form excitatory synapses (23). The β-neurexin/neurologin interaction induces the assembly of the postsynaptic machinery of excitatory and inhibitory synapses (24–26). However, these cases do not necessarily explain pathway specificity within a single neuron as clearly as netrin-Gs/NGLs because of promiscuous ligand–receptor interaction. Netrin-G1/NGL-1 and netrin-G2/NGL-2 interactions provide the molecular mechanisms that extrinsically determine pathway/lamina-specific properties of the subdendritic segments. The one-to-one relationship of the netrin-G/NGL interaction is advantageous for avoiding interference between adjacent neural pathways that converge onto a single neuron.

Which events are regulated by netrin-G/NGL interactions? NGL-1 and -2 have conserved amino acid sequences at the cytoplasmic C-terminal tail, which is a putative PDZ domain-binding motif. Indeed, various PDZ-like proteins interacting with NGLs were identified by yeast two-hybrid screening. These include members of the PSD-95 family (15), which are postsynaptic scaffold proteins involved in the recruitment of neurotransmitter receptors and associated signaling molecules (27, 28), and Whirlin, an adaptor protein involved in organization of the actin cytoskeleton (29, 30) that might regulate morphogenesis and/or stabilization of actin-rich structures, such as dendritic spines. Netrin-Gs might maintain the balance of distribution and activities of these synaptic machineries in a pathway-specific manner through their cognate receptors. In support of this idea, Kim *et al.* (15) demonstrated that direct clustering of NGL-2 induces the assembly of glutamatergic postsynaptic proteins and regulates the number of excitatory synapses in cultured neurons. In *Ntng1* KO and *Ntng2* KO mice, however, we found no significant differences in the density of PSD-95 clusters in any hippocampal layer under basal conditions (SI Fig. 10). It remains to be examined whether netrin-G/NGL interactions regulate other postsynaptic proteins that are more specific to layers, or whether recruitment of such molecules to the specific layers are induced by neural activity at specific pathways. In addition, as NGL-2 promotes presynaptic differentiation in cultured neurons probably through netrin-G2 (15), netrin-G mutant mice might also have deficits in presynaptic functions in a pathway-specific manner. These issues need to be investigated in future studies.

Finally, full sets of netrin-Gs and their receptor orthologues are conserved in all vertebrates, but not in the invertebrates so far examined, indicating that the netrin-G and NGL family members coevolved and contribute to higher brain functions. The distribution patterns of netrin-Gs can be roughly summarized as follows: netrin-G1 is distributed along the sensory relay projections to the cortices. Netrin-G2 is mainly distributed along intracortical (including intrahippocampal) connections. Netrin-G1 and -G2 might therefore differentially contribute to information processing, such as netrin-G1 to sensory perception and netrin-G2 to higher functions, such as memory formation. Studies in humans suggest the possible involvement of netrin-G1 and -G2 in schizophrenia, Rett syndrome, and bipolar disorder (31–33). Comparative analyses of the mutant mouse lines generated here will help to understand the role of lamina structures in the integration of distinct types of information, and to identify the neural circuits responsible for the symptoms of human brain diseases.

Materials and Methods

All experimental protocols were approved by the RIKEN Institutional Animal Care and Use Committee.

Immunohistochemistry. Rabbit polyclonal antibodies against netrin-G1 and -G2 were used as described in ref. 9. Antibodies to mouse NGL-1 and -2 were developed by immunizing rabbits with synthetic peptides, CNHYNSYKSPFNHTTTVNT (amino acid 596–613) for NGL-1 and CSEPYIIQTHTKDKVQE (amino acids 634–649) for NGL-2. Fresh frozen sections fixed with cold methanol were used for staining.

***In Situ* Hybridization.** Probes for *Ntng1* and *Ntng2* and preparation of digoxigenin-labeled antisense riboprobes were described in ref. 9. The *Ngl1* probe sequence contained a 5′ UTR and an N-terminal portion (nucleotides 467–1,057 of GenBank acces-

sion no. AK032467), whereas the *Ngl2* probe contained a C-terminal portion and a 3′ UTR (nucleotides 1,950–2,548 of GenBank accession no. AF290542). Hybridization of free-floating sections was performed according to the procedures described in ref. 34.

Cell Surface Binding Assay and BIAcore Analysis. Binding assay in HEK293T cells was performed as described in ref. 8. Quantitative analysis of binding affinity was performed on the BIAcore 2000 biosensor according to the manufacturer's instructions. Details are described in *SI Methods*.

Generation of Mutant Mice. For *Ntng1* disruption, the 246-bp genomic sequences encoding signal peptides and one-fourth of domain VI were replaced with *N-lacZ* and *loxP-pgk-neo-loxP* cassettes (35). *N-lacZ*, the *lacZ* gene with a nuclear localization signal, was ligated to the initiation codon of the *Ntng1* in frame. The *Ntng2* targeting vector was constructed by replacing the 1.3-kb KpnI–BglII fragment with a *loxP-pgk-neo-loxP* cassette. The deleted sequences contained a part of the 5′ UTR and encoded the signal peptide and one-fourth of domain VI. The E14 embryonic stem cell line was used for gene targeting (36). The heterozygous mutants were maintained by backcrossing with C57BL/6J and then interbred to obtain wild-type and mutant homozygotes. Mouse genotypes were determined by PCR using primers as follows: Ntng1-1 (5′-GTCAAGATTCCTGTCGATCC-3′), Ntng1-2 (5′-AGGGTCTC-CACAGGTAATATCC-3′), LacZ1 (5′-TCGGCGGTGAAAT-TATCGATGAGC-3′), and LacZ3 (5′-CCACAGCGGATGGTT-CGGATAATGC-3′). Primer pairs of Ntng1-1/Ntng1-2 and LacZ1/LacZ3 yielded 206-bp and 374-bp fragments from the wild-type and *Ntng1* KO allele, respectively. Ntng2-1 (5′-CTCTTCACAAT-GAAAGCCAAG-3′), Ntng2-2 (5′-TGAAGATAACACG-GAATCAGG-3′), and Ntng2-3 (5′-GGAGGGTAACCTTGCA-GATAG-3′) were used for genotyping the *Ntng2* KO line. Ntng2-1/Ntng2-2 and Ntng2-1/Ntng2-3 amplified 322-bp and 166-bp fragments from the wild-type and *Ntng2* KO allele, respectively. Histologic methods are given in *SI Methods*.

We thank the staff of the Research Resources Center of the RIKEN Brain Science Institute for technical support; T. Miyashita for advice on *in situ* hybridization and tracer experiments; T. Iwasato, Y. Yoshihara, K. S. Rockland, and N. Ichinohe for critical reading of the manuscript; and T. Onodera and C. Itakura for encouragement. This work was supported in part by the Special Postdoctoral Researchers Program of RIKEN (S.N.-A.), a Grant-in-Aid for Young Scientists from the Ministry of Education, Culture, Sports, Science, and Technology (to S.N.-A.), and the Strategic Programs for Research and Development from RIKEN (S.I.).

1. Sanes JR, Yamagata M (1999) *Curr Opin Neurobiol* 9:79–87.
2. Witter MP (1993) *Hippocampus* 3:33–44.
3. Skutella T, Nitsch R (2001) *Trends Neurosci* 24:107–113.
4. Otmakhova NA, Otmakhov N, Lisman JE (2002) *J Neurosci* 22:1199–1207.
5. Arrigoni E, Greene RW (2004) *Br J Pharmacol* 142:317–322.
6. Lorincz A, Notomi T, Tamas G, Shigemoto R, Nusser Z (2002) *Nat Neurosci* 5:1185–1193.
7. Nicholson DA, Trana R, Katz Y, Kath WL, Spruston N, Geinisman Y (2006) *Neuron* 50:431–442.
8. Nakashiba T, Ikeda T, Nishimura S, Tashiro K, Honjo T, Culotti JG, Itohara S (2000) *J Neurosci* 20:6540–6550.
9. Nakashiba T, Nishimura S, Ikeda T, Itohara S (2002) *Mech Dev* 111:47–60.
10. Yin Y, Miner JH, Sanes JR (2002) *Mol Cell Neurosci* 19:344–358.
11. Livesey FJ (1999) *Cell Mol Life Sci* 56:62–68.
12. Ishii N, Wadsworth WG, Stern BD, Culotti JG, Hedgecock EM (1992) *Neuron* 9:873–881.
13. Serafini T, Kennedy TE, Gaiko MJ, Mirzayan C, Jessell TM, Tessier-Lavigne M (1994) *Cell* 78:409–424.
14. Lin JC, Ho WH, Gurney A, Rosenthal A (2003) *Nat Neurosci* 6:1270–1276.
15. Kim S, Burette A, Chung HS, Kwon S-K, Woo J, Lee HW, Kim K, Kim H, Weinberg RJ, Kim E (2006) *Nat Neurosci* 9:1294–1301.
16. Herkenham M (1980) *Science* 207:532–535.
17. Schwob JE, Price JL (1984) *J Comp Neurol* 223:203–222.
18. Inaki K, Nishimura S, Nakashiba T, Itohara S, Yoshihara Y (2004) *J Comp Neurol* 479:243–256.
19. Witter MP, Amaral DG (2004) in *The Rat Nervous System*, ed Paxinos G (Elsevier Academic, San Diego), pp 635–704.
20. Ango F, di Cristo G, Higashiyama H, Bennett V, Wu P, Huang ZJ (2004) *Cell* 119:257–272.
21. Lin W, Burgess RW, Dominguez B, Pfaff SL, Sanes JR, Lee K-F (2001) *Nature* 410:1057–1064.
22. Kummer TT, Misgeld T, Sanes JR (2006) *Curr Opin Neurobiol* 16:74–82.
23. Dalva MB, Takasu MA, Lin MZ, Shamah SM, Hu L, Gale NW, Greenberg ME (2000) *Cell* 103:945–956.
24. Graf ER, Zhang X, Jin S-X, Linhoff MW, Craig AM (2004) *Cell* 119:1013–1026.
25. Chih B, Engelman H, Scheiffele P (2005) *Science* 307:1324–1328.
26. Nam CI, Chen L (2005) *Proc Natl Acad Sci USA* 102:6137–6142.
27. Kim E, Sheng M (2004) *Nat Rev Neurosci* 5:771–781.
28. Montgomery JM, Zamorano PL, Garner CC (2004) *Cell Mol Life Sci* 61:911–929.
29. Delprat B, Michel V, Goodyear R, Yamasaki Y, Michalski N, El-Amraoui A, Perfettini I, Legrain P, Richardson G, Hardelin J-P, *et al.* (2005) *Hum Mol Genet* 14:401–410.
30. Mburu P, Mustapha M, Varela A, Weil D, El-Amraoui A, Holme RH, Rump A, Hardisty RE, Blanchard S, Coimbra RS, *et al.* (2003) *Nat Genet* 34:421–428.
31. Aoki-Suzuki M, Yamada K, Meerabux J, Iwayama-Shigeno Y, Ohba H, Iwamoto K, Takao H, Toyota T, Suto Y, Nakatani N, *et al.* (2005) *Biol Psychiatry* 57:382–393.
32. Borg I, Freude K, Kubart S, Hoffmann K, Menzel C, Laccone F, Firth H, Ferguson-Smith MA, Tommerup N, Ropers H-H, *et al.* (2005) *Eur J Hum Genet* 13:921–927.
33. Eastwood SL, Harrison PJ (May 16, 2007) *Neuropsychopharmacology*, 10.1038/sj.npp.1301457.
34. Miyashita T, Nishimura-Akiyoshi S, Itohara S, Rockland KS (2005) *Neuroscience* 136:487–496.
35. Sassa T, Gomi H, Itohara S (2004) *Cell Tissue Res* 315:147–156.
36. Hooper M, Hardy K, Handyside A, Hunter S, Monk M (1987) *Nature* 326:292–295.